JOURNAL OF MATERIALS SCIENCE **38** (2003) 2995–3005

Review
Formation, microstructural characteristics and stability of carbon supported platinum catalysts for low temperature fuel cells

E. ANTOLINI
Scuola di Scienza di Materiali, Via 25 Aprile 22, 16016 Cogoleto (Genova), Italy
E-mail: ermantol@libero.it

Supported platinum electrocatalysts are generally used in low temperature fuel cells to enhance the rates of the hydrogen oxidation and oxygen reduction reactions. In such catalysts, the high surface to volume ratios of the platinum particles maximize the area of the surfaces available for reaction. It is the structure and proper dispersal of these platinum particles that make low-loading catalysts feasible for fuel cell operation, lowering the cost of the system. If the platinum particles cannot maintain their structure over the lifetime of the fuel cell, change in the morphology of the catalyst layer from the initial state will result in a loss of electrochemical activity. This loss of activity in the platinum/carbon catalysts due to the agglomeration of platinum particles is considered to be a major cause of the decrease in cell performance, especially in the case of the cathode. In the light of the latest advances on this field, this paper reviews the preparation methods of these catalysts, their microstructural characteristic and their effect on both thermal and in cell conditions stability.

1. Introduction

Highly dispersed platinum crystallites on a conductive support such as high surface area carbon powders are used as catalysts for hydrogenation and oxidation reactions. Carbon supported platinum (Pt/C) is the best known electrocatalyst for both hydrogen oxidation and oxygen reduction in phosphoric acid fuel cells (PAFCs) and proton exchange membrane fuel cells (PEMFCs). The structure and proper dispersal of these platinum particles make low loading catalyst feasible for PAFC and PEFC operation. If the platinum particles cannot maintain their structure over the lifetime of the fuel cell, change in the morphology of the catalyst layer from the initial state will result in a loss of electrochemical activity.

Pt/C is also used to obtain carbon-supported platinum/metal alloys (PtM/C). As reported in a previous review on the formation of PtM/C [1], these catalyts are obtained by deposition of the less precious metal on the carbon supported platinum followed by alloying at high temperature. In this case, to reduce the sintering of Pt particles at alloying temperature, causing a decrease of catalytic activity, it is essential to improve the thermal stability of metal particles.

Mukerjee [2] reviewed the structural and particle size effects in platinum electrocatalysis, while Rodriguez-Reinoso [3] dealt with the surface chemistry of carbon supports and the influence of the oxygen groups on the carbon surface upon the properties of the supported catalysts. The purpose of this paper is to provide a better insight into the formation, microstructural characteristics and stability of these catalysts, in the light of the latest advances on this field.

2. Pt/C formation

The manufacture and the chemical and physical properties of carbons as supports for precious metal catalysts were reviewed by Auer *et al*. [4]. Generally, two characteristics have to be considered in the evaluation of carbon-supported metals: the microscopic distribution of metal crystallites on the support surface and the macroscopic distribution of metal particles in the individual support particles. The microscopic distribution of metal crystallites is referred to as dispersion or fraction exposed, and is in relation to metal particle size. Regarding the macroscopic distribution of the metal on the carbon support, it can be uniform or egg-shell. Mixed types between these extreme situations are possible. Two methods are generally used to obtain carbon supported platinum catalysts, (1) impregnation of carbon support with Pt precursor solution, and (2) adsorption of platinum oxide or platinum metal colloids onto the carbon surface. By the former mechanism, uniformly impregnated catalysts are available because an equilibrium between adsorbed and free ions exists and diffusion into the core of each individual support particle can occur. The latter mechanism can give rise to egg-shell distribution. The colloid particles adsorb on

the external surface of the support particles and in their macropores. Owing to the size of the colloid particles, the accessibility of the inner pores is very limited, leading to egg-shell distribution of the platinum.

2.1. Impregnation method

The catalyst is prepared by impregnating the carbon support of an aqueous solution of H_2PtCl_6 (in acid media) or $[Pt(NH_3)_4]Cl_2$ (in basic media), followed by platinum reduction, generally with flowing H_2 in the temperature range 200–350°C, but also with other reducing agents. Independent of the origin and the pore structure of the carbon, by a proper choice of the preparation conditions, a high platinum dispersion can be obtained [5]. According to a recent study of Fraga *et al.* [6], the specific surface area of the carbon support seems to have only a little effect on Pt dispersion.

2.1.1. Impregnation

The impregnation step has been extensively studied [6–12]. Pt reduction during the impregnation step was observed by several authors. Early X-ray photoelectron spectroscopy (XPS) studies [7] indicated that after impregnation of carbon with H_2PtCl_6 and subsequent drying in air, the platinum was present as Pt^0 and Pt^{2+}. Van Dam and van Bekkum [8] showed that upon impregnation into activated carbon, H_2PtCl_6 is partly converted into a Pt^{2+} complex. The presence of divalent platinum in the catalyst after impregnation was observed also by Coloma *et al.* [9]. According to Miguel *et al.* [10], the interaction of H_2PtCl_6 with the carbon implies a redox process in which after impregnation and drying the metal complex is stabilized as Pt^{2+} on the carbon surface. They found that the difference in the support surface chemistry seems to have no effect on the resulting state of platinum. Pt reduction during the impregnation process was confirmed by Fraga *et al.* [6] from combined XPS and temperature-programmed reduction (TPR) studies. The analysis of the adsorption isotherms of H_2PtCl_6 on activated carbon [8, 11] indicated that these isotherms cannot be described as a Langmuir type process, so revealing that Pt adsorption on the carbon support is not a simple process. All isotherms showed a first portion where H_2PtCl_6 is very strongly adsorbed, and a second portion where weak adsorption was denoted, independent of the surface chemistry of the carrier. The oxidative pre-treatment of the carbon decreased the strong adsorption of platinum [8]. As van Dam and van Bekkum [8] showed, a simple electrostatic mechanism cannot explain the adsorption process of H_2PtCl_6 on the different carbon supports. They proposed a model to describe the chemistry of the impregnation of hexachloroplatinic acid on carbon. First, carbon reduces the Pt(IV) complex to a Pt(II) complex, which is then coordinatively bound to the carrier, as:

$$H_2Pt(IV)Cl_6 + {-}C{-}H + H_2O \rightarrow Pt(II)Cl_4^{2-} + 2Cl^- + {-}CO^- + 5H^+ \quad (1)$$

$$Pt(II)Cl_4^{2-} + \underline{S} \rightarrow Pt(II)Cl_3\underline{S}^- + Cl^- \quad (2)$$

The ligand site $\underline{S}$ is assumed to be either a π-complex structure or an oxygen surface group. A model for an oxidized carbon surface would be based on independent acid and basic groups, which ionize according to the following equilibria:

$$H\underline{A} \leftrightarrow \underline{A}^- + H^+ \quad (3)$$

$$\underline{B} + H^+ \leftrightarrow BH^+ \quad (4)$$

where $\underline{A}$ and $\underline{B}$ denote sites of the carbon solid matrix or surface oxygen groups [13]. Thus, the combination of the model of van Dam and van Bekkum with the model for the ionisation behaviour of the carbon surface based on independent acid and basic groups leads to the conclusion that the acid oxygen surface groups should be considered as weak anchoring sites. On this basis, carbon surface basic sites act as anchoring sites for the hexachloroplatinic anion and are responsible for the strong adsorption of platinum on carbon. The nature of the carbon surface basic sites is still a subject of discussion. The carbon surface basic sites are frequently associated with pyrone-like structure. Such structures which have a $pK_b > 11$ and which decompose thermally at 777–927°C, generating CO [14, 15], would present a strong electronic interaction with the surface carboxyl groups, which leads to their destruction by surface oxidation [14]. According to other authors [16–18], the surface basic sites are essentially of Lewis type and are associated with π-electron rich regions within the basal planes. According to Leon y Leon *et al.* [18], the protonation of such oxygen-free basic carbon sites would lead to an electron-donor-acceptor complex, as the following:

$$C_\pi + H_3O^+ \leftrightarrow [C_\pi\text{-}H_3O]^+ \quad (5)$$

$$C_\pi + 2H_2O \leftrightarrow [C_\pi\text{-}H_3O]^+ + OH^- \quad (6)$$

where C_π is probably a graphitized carbon surface platelet in which single π electron pairs may become partially localized as a result of the H_3O^+ addition. In the model of van Dam and van Bekkum the two step of the strong adsorption of Pt, the reduction and the coordination of the platinum complex, are not directly connected, while the adsorption experiments show that H_2PtCl_6 reduction takes place simultaneously with its adsorption [8, 11]. Lambert and Che [19] proposed an alternative formulation of the model of van Dam and van Bekkum for the strong adsorption of $PtCl^{6-}$, using the mechanism of inner-sphere adsorption. This alternative model can be described by the following relations:

$$Pt(IV)Cl_6^{2-} + [C_\pi\text{-}OH_3]^+ \rightarrow [C{-}OH_2{-}Pt(IV)Cl_5]^- + HCl \quad \text{(adsorption of } PtCl_6^{2-} \text{ without reduction)} \quad (7)$$

$$Pt(IV)Cl_6^{2-} + [C_\pi\text{-}OH_3]^+ \rightarrow [C{-}O{-}Pt(II)Cl_3]^- + 3HCl \quad \text{(adsorption with simultaneous reduction)} \quad (8)$$

According to this model, surface groups would replace some of the original ligands (Cl^-) of the transition metal in solution. In the case of Equation 7, an insertion of a water ligand takes place, while for that regarding Equation 8 a C─O─Pt linkage would be formed. Being C_π-OH_3^+ one of the basic surface groups of carbon, as shown in Equations 5 and 6, the Equations 7 and 8 should not be taken as stoichiometric ones. Moreover, Fourier transform extended x-ray absorption fine structure (FT-EXAFS) analysis indicated that for some Pt/C catalysts prepared by impregnation with H_2PtCl_6 the strong interaction between the Pt precursor and the support is associated with a change in the Pt coordination from Cl to O atoms [20, 21]. Ageeva *et al.* [22] studied the mechanism and kinetics of the adsorption of platinum and other metals on activated carbon from chloride solutions exposed to ultraviolet (UV) radiation. They found that UV illumination does not change thermodynamic parameters of adsorption but affects the adsorption kinetics.

2.1.2. Effect of oxidative treatment of carbon

The functionalities present on the carbon surface in the form of surface oxides (e.g., carboxylic groups, phenolic groups, lactonic groups, etheric groups) are responsible both for the acid/base and the redox properties of the carbon [23]. The oxidative treatment of the carbon surface gives rise to the formation of surface acidic sites and to the destruction of surface basic sites. This treatment of carbon can be performed by different oxidants: HNO_3, H_2O_2, O_2 or O_3. The effect of oxidative pre-treatment of the carbon on platinum dispersion has produced contradictory results in literature data. According to some authors [11, 21, 24, 25], the dispersion increases with increasing the number of oxygen surface groups in the support. Torres *et al.* [11] showed that the effect of the different oxidants can be related to the nature of the functional groups on the carbon surface. HNO_3-treated carbon displays a high density of both strong and weak acid sites, while H_2O_2- and O_3-treated carbons show an important concentration of weak acid sites but a low concentration of strong acid sites. The H_2PtCl_6 isotherms in liquid phase at 25°C showed a stronger interaction of the metallic precursor with the carbon of low acidity (like those treated with H_2O_2 or O_3) than with the most acidic carbon (treated with HNO_3). Carbons functionalised with weak oxidants, which develop acidic sites with moderate strength and show strong interaction with H_2PtCl_6 during impregnation, would favour the Pt dispersion on the carbon surface. According to Sepulveda *et al.* [12], the presence of oxygen surface groups in the support favours the anchoring of $[Pt(NH_3)_4]^{2+}$, but does not affect the amount of platinum retained by the support when H_2PtCl_6 is used as metal precursor. They also showed that the oxidized support hinders the reduction of the Pt precursor. Other authors [9, 20, 26, 27], instead, reported that the presence of oxygen surface groups on carbon decreases the metal dispersion. Microcalorimetric measurements of CO adsorption performed by Guerrero-Ruiz *et al.* [27] evidenced that the presence of oxygen

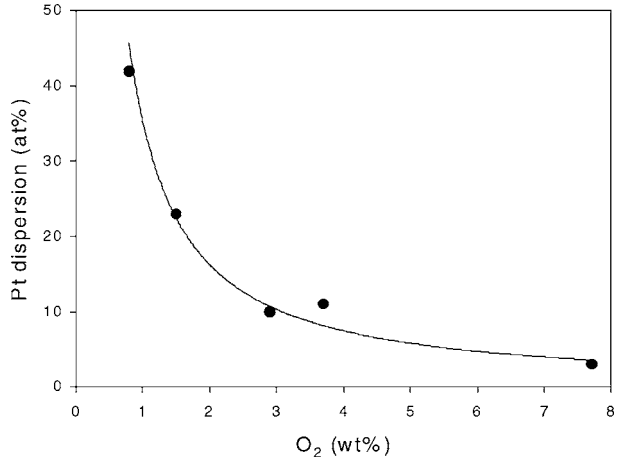

Figure 1 Dependence of platinum dispersion in Pt/C catalysts on total surface oxygen content of the support [6].

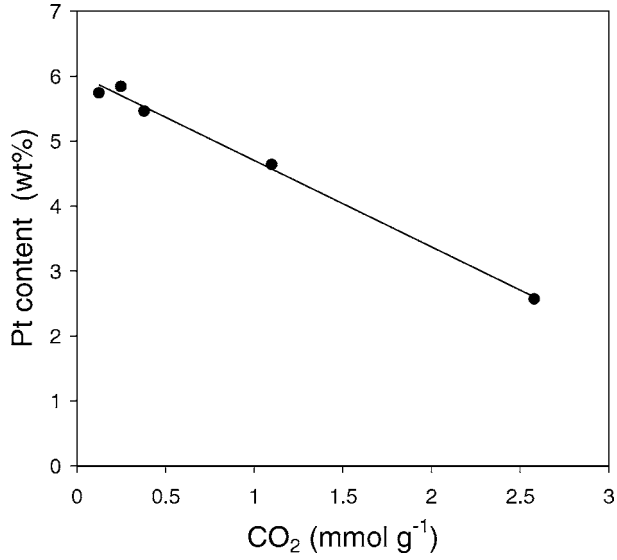

Figure 2 Dependence of platinum content in Pt/C catalysts on CO_2 amount in TPD spectra of the support [6].

surface groups diminishes the metal-support interaction. In Fig. 1 we can see the plot of Pt dispersion, obtained by H_2 chemisorption, vs. O_2, the total surface oxygen content of the support, from Fraga *et al.* [6]. According to the authors, the decrease in the dispersion, calculated by assuming a stoichiometry (H:Pt) of 1:1, with the increase in the total surface oxygen is due to the reduction of the number of surface basic sites, which are centers for the strong adsorption of $PtCl_6^{2-}$. Fig. 2 shows the dependence of Pt amount in the catalyst on the acidity of the support, as defined by the CO_2 value of temperature-programmed desorption (TPD) spectra of the supports [6]. The platinum content in the catalyst also depends on the oxidative treatment of carbon and linearly decreases with increasing CO_2 of the support.

2.2. Colloidal method

The method consists in the preparation of a platinum metal colloid, followed by adsorption on the carbon support, or in the formation of a Pt oxide colloid, followed by simultaneous reduction and adsorption, or adsorption followed by reduction.

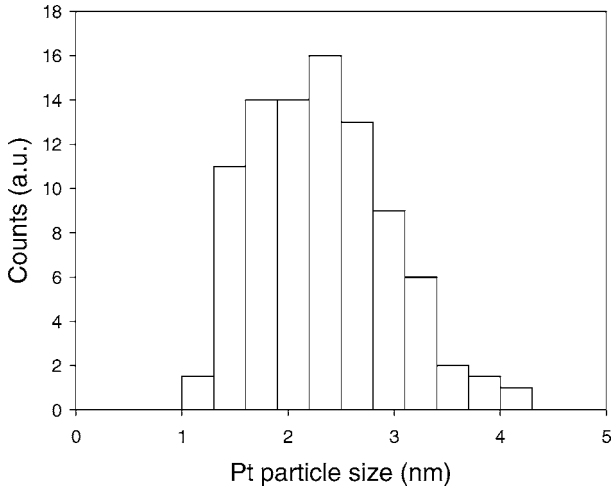

Figure 3 Particle size distribution for E-TEK 20 wt% Pt/C catalyst [30].

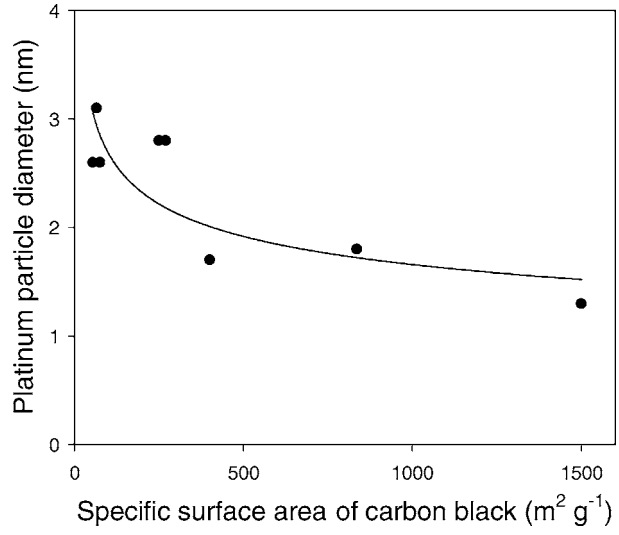

Figure 4 Platinum particle diameter vs. specific surface area of carbon black [38].

2.2.1. Fabrication routes

The sulfite-complex route [28, 29] consists of the synthesis of Pt sulfite complexes in aqueous solution starting from H_2PtCl_6 and $NaHSO_3$, oxidative decomposition of the complex by H_2O_2 addition with simultaneous adsorption onto the carbon black suspended in the solution. Then, after water washing the catalyst is reduced in flowing hydrogen at 300°C. The particle size distribution from transmission electron microscopy (TEM) analysis of 20% Pt/C catalyst prepared by E-TEK using this method was monomodal in the range 1.2 to 4.3 nm with a tail in the region of the larger sizes, as shown in Fig. 3 [30]. The mean value of particle size was 2.6 nm.

The preparation method of Pt/C developed by Giordano *et al*. [31] is based on the liquid-phase reduction of H_2PtCl_6 with an excess of $Na_2S_2O_4$. The temperature of the H_2PtCl_6 solution is raised to 60°C, and H_2O_2 is added to stabilize the colloidal suspension. Then, the $Na_2S_2O_4$ solution is added dropwise to form the colloidal Pt particles. A suspension of these particles is added to a slurry of carbon black to form the supported catalyst.

The alcohol reduction method [32–34] has been widely used in the formation of metal colloids for the preparation of both homogeneous and heterogeneous catalysts. The catalysts are prepared by the reduction of H_2PtCl_6 with methyl alcohol in the presence of a surface-active agent and a carbon support [35, 36]. The resulting suspension is stirred and heated in the temperature range 60-80°C to reduce the chloroplatinic acid and to support the platinum particle onto the carbon black.

McBreen *et al*. [37] investigated the effect of the carbon support on the Pt dispersion in Pt/C catalysts obtained by the colloidal method. Of the five carbon blacks used in their study, Vulcan XC-72 and Regal 600R yielded a higher Pt dispersion than that obtained with Monarch 1300, CSX98 and Mogul L. These results were attributed to the high internal porosity of Vulcan XC-72 which serves to enhance Pt dispersion. On the other hand, the high Pt dispersion on Regal 600R is attributed to the surface properties of the carbon which results in a strong Pt-carbon interaction.

Uchida *et al*. [38] evaluated the effect of the specific surface area of different carbon on Pt particle size of Pt/C catalysts obtained by the sulfite-complex method. As shown in Fig. 4, Pt particle size decreased with increasing the specific surface area of carbon black. The same result was obtained by Watanabe *et al*. [39, 40]. It seems that Pt particle size grew larger because the number of the Pt oxide colloid particles that were adsorbed onto a surface of the supported platinum increased with a decrease of the specific surface area of the carbon support. On the other hand, the number of the Pt oxide colloid particles that were adsorbed on a surface of the carbon support increased with increasing specific surface area of the support.

Honji *et al*. [41] prepared Pt/C catalysts by the alcohol reduction method using sorbitan monolaurate as surface-active agent. This dispersing agent, unlike polyoxyethylene glycol p-iso-octylphenyl ether [35], prevents the formation of platinum colonies on carbon support. The catalysts were thermal treated at 350°C in N_2 to decompose the residual surface-active agent. They studied the effect of the concentration of sorbitan monolaurate to optimise the preparation condition. The dependence of Pt particle size on the concentration of sorbitan monolaurate, before and after heat treatment at 350°C, is shown in Fig. 5. Before heat treatment, platinum particle diameter slightly decreased with increasing sorbitan monolaurate concentration, while after thermal treatment Pt particle grew from 3.4 nm to 4.7 nm by decreasing surface-active agent concentration from 5 to 2.5 g l^{-1}.

The effect of thermal treatment temperature of the suspension on platinum particle size in the catalyst preparation by the alcohol reduction method was investigated by Wang and Hsing [36]. They used as the dispersing agent dodecyldimethyl (3sulfo-propyl) ammonium hydroxide (SB12). Different from the polymer based stabilizer (steric effect), the stabilization mechanism of SB12 surfactant is probably related to an electrostatic effect [42]. As shown in Fig. 6, the size of Pt particles decreases with increasing synthesis temperature. This effect can be explained by the theory of

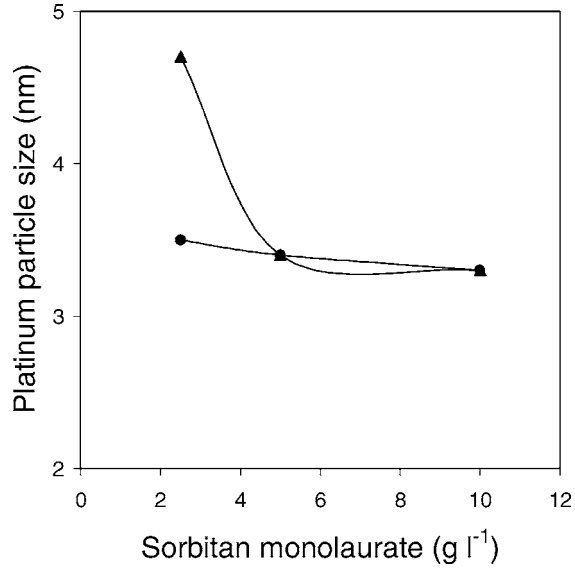

Figure 5 Dependence of platinum particle size on sorbitan monolaurate concentration: (●) before and (▲) after thermal treatment at 350°C for 3 h in N_2 [41].

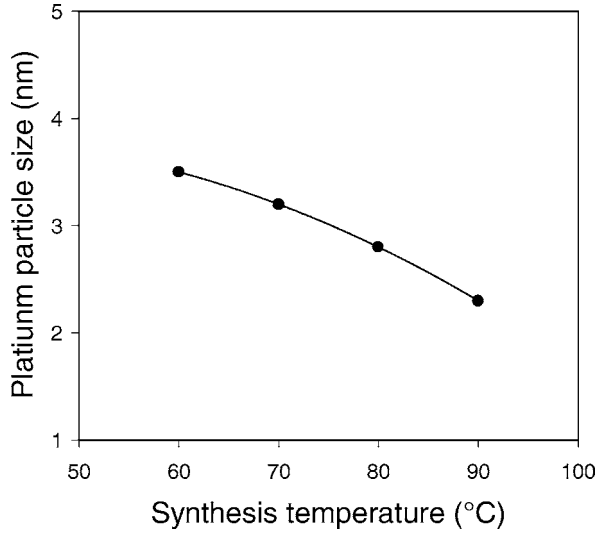

Figure 6 Platinum crystallite size vs. synthesis temperature [36].

crystallization. The rate of nucleation determines the number and size of the primary particles generated in a supersaturated solution. The higher the reaction rate (i.e., higher temperature), the higher the supersaturation, consequently the number of nuclei is larger and the size can be smaller. It is known [30] that a remarkable growth of particle size takes place when preparing high loading electrocatalysts. In the preparation method of Wang and Hsing [36], instead, the loading shows little effect on the particle size as the colloid is pre-formed in the solution and the loading is determined by the amount of carbon added. The particle sizes of carbon supported platinum for various Pt loadings by E-TEK and Wang and Hsing, respectively, are listed in Table I.

2.3. Reduction

Platinum reduction following the impregnation or adsorption step can be carried out by different methods: heating in flowing hydrogen in the temperature range 300–500°C, electrochemical reduction in H_2SO_4,

TABLE I Platinum particle size (nm) of Pt/C catalysts with different Pt loadings

Pt loading (wt%) (Pt/C)	Pt particle size by E-TEK [30]	Pt particle size by Wang and Hsing [36]
20	2.4	2.5
30	3.2	/
40	3.9	2.5

chemical reduction with N_2H_2, $NaBH_4$ or $Na_2S_2O_4$. The reduction of platinum is not quantitative and a small fraction of oxide species always remains on the carbon support. Miguel *et al.* [10] found that, during thermal treatment in H_2, apart from the reduction of Pt species to Pt^0, catalysed and non-catalysed reactions involving CO and CO_2 desorbed from the carbon surface, took place. They also found that the Pt^{2+} species were reduced to zerovalent Pt following thermal treatment in He. Stoyanova *et al.* [43] found that the reduction method affects the kind of crystal faces exposed at the particle surface, the particle size and the partial oxidation of the carbon support. If the reduction takes place in a liquid environment (as in the case of the chemical reduction with N_2H_2, $Na_2S_2O_4$ or $NaBH_4$ solutions), Pt precursors dissolution could occur simultaneously with reduction, affecting the dispersion of the catalyst. $Na_2S_2O_4$ is a weak reducing agent [44]. It reacts with the chloroplatinic ions to form finely divided metal particles having a large surface area. It seems that in this reaction finely divided sulfur may be formed by decomposition of the sulfur-precursor according to the following equation, which is known to occur in an acidic solution:

$$S_2O_4^{2-} + 2H^+ \rightarrow H_2S_2O_4 \rightarrow S + H_2SO_4 \quad (9)$$

The sulfur particles thus obtained serve as nuclei for growing finely divided metal catalyst particles, depending on carbon characteristics [45]. In the case of non-activated Vulcan XC-72R carbon, weak carbon surface-metal precursor interactions take place during impregnation, so Pt crystallites nucleate and grow on sulfur particles, formed during reduction. Owing to the high number of S particles, the Pt dispersion is high, resulting in small Pt aggregates. In the case of Ketjenblack type carbon, instead, the presence of basic sites on the carbon surface plays an important role in the adsorption of H_2PtCl_6, by undergoing a strong interaction with it [46]. During reduction the crystallites nucleates and grow on some of these sites. The Pt^{2+} reduction on the crystallite surface being the rate limiting step ($Na_2S_2O_4$ is a weak reducing agent, the Pt^{2+} diffusion is relatively fast), the growth rate of a crystallite will be proportional to its surface area. So, large crystallites will grow faster than small crystallites. This finally results in a small number of large crystallites.

2.4. Thermal activation

Following reduction, thermal activation of the catalyst is performed by some authors under a flowing N_2 or Ar at 110–900°C for times ranging from 1 to 4 h. Heat treatment at 900°C in an atmosphere of nitrogen was

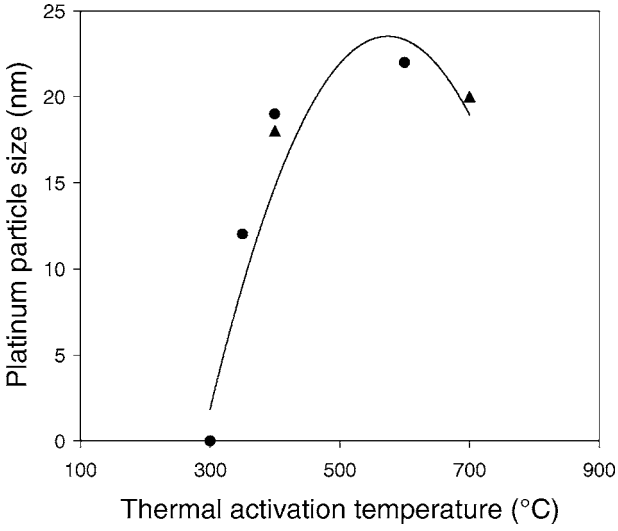

Figure 7 Dependence of platinum particle size from (●) XRD and (▲) TEM measurements on thermal activation temperature [45].

carried out by Jalan *et al.* [47, 48]. This treatment causes the platinum particles to grow from a wide dispersed particle size in the range 1.5–3.5 nm to an uniform particle size of mean value 4.2 ± 0.5 nm with fairly normal distribution. Moreover, the thermal treatment gives rise to an uniform distribution of platinum over the carbon particles. Torre *et al.* [46] investigated the events occurring during thermal activation of Pt/C catalysts by various techniques (potentiometric titration determining the zero point of charge (ZPC), FT-IR, TPD and XPS). Their results suggest that surface acidic oxygen-containing functional groups may act as anchoring centres for the metal particles limiting their growth in the low-temperature range. This effect produces a strong metal-support interaction which affects the electronic nature of platinum sites. In the high-temperature range, basic functional groups are mainly individuated, i.e., C_π- and pyrone-type sites. Pyrone groups behave similarly to the acidic groups whereas C_π groups possess an electron-releasing behaviour producing a lower level of metal-support interaction.

Using $Na_2S_2O_4$ as reducing agent and Vulcan XC-72R carbon as platinum support, the formation of small Pt particle occurs, as indicated earlier. Thermal treatment in Ar of this catalyst gives rise to Pt particle growth at low temperatures [45]. On the basis of the data reported in [45], the dependence of Pt particle size on thermal treatment temperature is shown in Fig. 7. The coalescence of Pt particles almost completely occurred in the temperature range 300-400°C. In this case sulfur presence can support the sintering of Pt particles at relatively low temperatures, as denoted by a study of Pt clusters in zeolite after poisoning with sulfur [49]. In the presence of sulfur, Pt mobility on carbon takes place by a different route, S enables Pt atoms to move by a bridge-bonding mechanism [50].

3. Microstructural characteristics

XRD analysis by Mukerjee *et al.* [51] showed that the 2θ positions of the ⟨100⟩, ⟨111⟩, ⟨200⟩ and ⟨220⟩ powder diffraction lines for carbon supported platinum compare well with the standard JCPDS powder diffraction files, thus indicating that Pt/C has face-center cubic (fcc) crystal structure similar to bulk Pt. The cubic lattice parameter is in agreement with that in bulk metal [52].

X-ray absorption near-edge structure (XANES) provides information on the Pt d-band vacancies. The d-band vacancies are derived from an analysis of the Pt L_3 and L_2 white lines. The respective L_3 and L_2 edges are due to excitation of $2p_{1/2}$ and $2p_{3/2}$ electrons. The Pt L_3 XANES for Pt foil and carbon supported Pt in 1 M HClO4, at 0.54 V, are identical [51]. The calculated value of the Pt d-orbital vacancy per atom is 0.329 for both bulk and carbon-supported platinum.

Electronic interaction between platinum and carbon has been recognized by electron-spin resonance (ESR) and XPS studies. ESR analysis has demonstrated electron donation by platinum to carbon support [53]. This result was confirmed by an XPS study performed by Escard *et al.* [54]. The XPS Pt 4 $f_{7/2}$ peak for the Pt/C catalyst shifted to higher values by 0.4 eV with respect to unsupported platinum [30], according to previous studies on zeolite-supported [55] and carbon-supported platinum [56]. This result was interpreted as related to the presence of a platinum-support electronic effect. The specific metal-support interaction is through electron transfer from platinum to clusters to oxygen atoms of the surface of the support. When two solids are joined to form an adhesive couple, the adhesion properties of the couple depend on the morphological, chemical and physical nature of their interface [57]. In the absence of material mixing and mechanical interlocking, the adhesion is intrinsic in nature and arises from molecular, electrostatic or chemical surface forces acting across the interface of two dissimilar substances. In many cases, chemical bonds are formed or charge transfer takes place between the contacting phases. There is also a small-particle effect [58–60]: particles in the 1–2 nm range have not yet attained the normal bulk band structure, so the binding energy for the particles shifts to higher values.

Extended x-ray absorption fine structure (EXAFS) gives information on the coordination number of bulk and carbon-supported platinum. The Pt/C electrocatalyst shows a coordination number of 9 instead of 12 (bulk Pt) [51]. The primary reason for this behaviour is based on the particle size of Pt crystallites. The particle size has an effect on the relative fraction of Pt surface atoms on the ⟨111⟩ and ⟨100⟩ faces of the Pt particle [61]. Romanovski [62] suggested that a minimum surface energy is obtained for Pt particles that have a cubo-octahedral structure. An early study of Jalan [63] by high-resolution transmission electron microscopy (HRTEM) reported the presence of carbon-supported platinum particles of around 4 nm diameter having a two-dimensional shape (flat, raft like, disk like). However, these shapes are not likely to be present in Pt/C particles thermally treated at elevated temperatures. Another study by HRTEM measurements on carbon-supported platinum, instead, indicated the presence of Pt particles having cubo-octahedral structure [64]. A study on Pt/C by scanning tunnelling microscopy

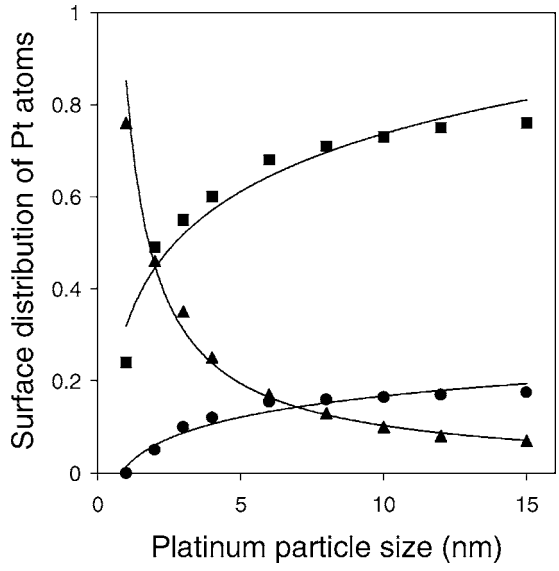

Figure 8 Surface distribution of Pt atoms: (●) ⟨100⟩ atoms, (■) ⟨111⟩ atoms, (▲) edge and corner atoms [61].

(STM) provided further evidence of the presence of cubo-octahedral geometry for supported platinum particles in the range of 3–4 nm diameter [65]. The cubo-octahedral particles consist of eight octahedral ⟨111⟩ crystal faces and six cubic ⟨100⟩ crystal faces bounded by edge and corner atoms. The relationship between the Pt particle size and number of atoms associated with the ⟨111⟩ and ⟨100⟩ crystal faces and the edge and corner sites can be predicted by the analysis of Van Hardeveld *et al.* [66, 67]. Regardless of the preparation method, it is unlikely that Pt particles which consist of ⟨111⟩ and ⟨100⟩ crystal faces and edge and corner sites of the ideal cubo-octahedral structure are formed. This means that crystal faces besides the ⟨111⟩ and ⟨100⟩ orientations are formed on the cubo-octahedral structure and they are created by the addition of atoms to existing crystal faces. The surface sites that are associated with B_5 sites (the ⟨111⟩ and ⟨100⟩ crystal faces are B_3 and B_4 sites, respectively) [66, 67], for example ⟨110⟩ and ⟨113⟩ crystal faces, are likely to form on particles that do not contain the exact number of atoms to produce complete cubo-octahedral structure. The analysis by Van Hardeveld *et al.* indicated that B_5 sites represent only a small fraction of the total atoms in Pt particles that are less than about 1.5 nm and larger than about 8 nm. However, for particles between these two particle diameters, the mass-averaged distribution of B_5 sites could reach a maximum of about 15%. Fig. 8 from [61] shows the distribution of surface atoms on the ⟨111⟩ and ⟨100⟩ crystal faces and the edge and corner sites, normalized to the total number of atoms on the surface of the particle. The number of atoms on the ⟨111⟩ and ⟨100⟩ faces increases as the particle size increases. On the other hand, the number of atoms on the edge and corner sites decreases rapidly with increasing particle size.

4. Stability in PAFC and PEFC condition

Platinum particle sintering takes place in Pt/C catalysts during cell operation in PAFCs. Table II shows Pt particle size following different times of PAFC operation.

TABLE II Platinum particle size following different times of PAFC operation

Cell operation time (h)	Pt particle size [35] (nm)	Pt particle size [72] (nm)	PtCo particle size [72] (nm)
0	3.8	3.4	12.0
20	9.5–10.5		
50	9.5–10	8.1	13.5
100	11.0–12.0		

As can be seen in Table II, platinum growth rate is high for small particles, likely by the higher solubility in phosphoric acid of edge and corner atoms with respect to ⟨111⟩ and ⟨100⟩ atoms, and above 10 nm the size tends to stabilize. Many studies have been devoted to evaluating the mechanism of platinum particle agglomeration in phosphoric acid (PAFC condition) [35, 68–71]. Essentially, two mechanisms have been proposed to explain the surface area loss of carbon-supported platinum: (1) dissolution/reprecipitation [35, 68, 70] and (2) surface diffusion [69, 71]. In the former case, the platinum dissolves in hot phosphoric acid, then, following the saturation of electrolyte with platinum ions, Pt redeposition takes place. The effect of pH of the liquid environment in Pt particle growth was observed by Beard and Ross [72]. They prepared carbon-supported PtCo alloy by adding Pt/C catalyst at room temperature into two cobalt solutions, at pH 2 and 11, respectively. When the supported Pt was added into the solution at pH 11, the platinum particle size only slightly changed, while in the case of the solution at pH 2 a remarkable particle growth was denoted, from 2.5 to 3.4 nm. Thus it seems that the acidic solution affects the high-surface-area Pt particle by a dissolution/deposition process since, according to Pourbaix [73], Pt is slightly soluble in acidic environment. As denoted by Hyde *et al.* [74], following 4500 h of cell operating about 10 wt% of the platinum was lost from the cathode and migrated across the phosphoric acid to the anode, supporting as a consequence the dissolution/redeposition mechanism. As Honji *et al.* [35], Pt particle growth in phosphoric acid is noticeably larger in the presence of air than in the presence of nitrogen.

In the latter case, the area loss of supported platinum occurs by surface diffusion of crystallites [69, 71] or migration of platinum atoms on the carbon surface [75]. This hypothesis is based on the following experimental results. Bett *et al.* [75] found that the nature of the liquid environment seems to have no effect on Pt sintering. Many studies [9, 11, 20, 21, 24–27, 69] showed that the resistance to sintering is related to the presence of surface oxygen groups, which interact with the movement of Pt particle on the carbon surface. As in the case of Pt dispersion, conflicting results on the effect of oxidative pre-treatment were reported.

The effect of electrode potential on Pt particle growth produced contradictory results. Stonehart *et al.* [76] investigated the dependence of the sintering of unsupported platinum on potential. They found that the rate of agglomeration is greatest at low and smallest at high potentials. For that regarding carbon-supported platinum, Bett *et al.* [75] and Gruver *et al.* [71] found that the

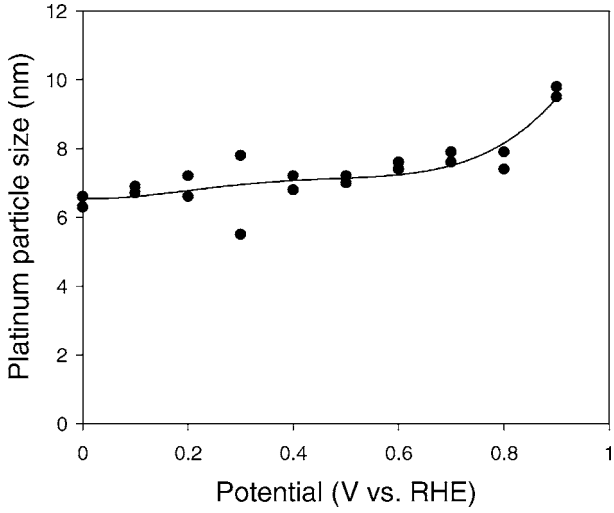

Figure 9 Effect of potential on platinum particle size [35].

electrode potential has only a small effect on the crystallite growth rate. Honji *et al.* [35], instead, observed a potential dependence of the Pt sintering. As shown in Fig. 9, unlike the result of Stonehart *et al.* for Pt black [76], the particle size increases with increasing the potential, particularly at 0.90 V vs. reversible hydrogen electrode (RHE). Finally, Meyers and Darling [77] showed that Pt dissolution in polymer electrolyte fuel cells is negligible at low and high potentials, but is remarkable at intermediate potentials. In their kinetic model of Pt dissolution in PEFCs, they explained the effect of potential in the following way. They considered three reactions:

$$\mathrm{Pt} \rightarrow \mathrm{Pt}^{2+} + 2\mathrm{e}^{-} \text{ (platinum dissolution)} \tag{10}$$

$$\mathrm{Pt} + \mathrm{H_2O} \rightarrow \mathrm{PtO} + 2\mathrm{H}^{+} + 2\mathrm{e}^{-} \text{ (platinum oxide film formation)} \tag{11}$$

$$\mathrm{PtO} + 2\mathrm{H}^{+} \rightarrow \mathrm{Pt}^{2+} + \mathrm{H_2O} \text{ (chemical dissolution of platinum oxide)} \tag{12}$$

The reaction (12) is assumed to be slow, but is necessary for the model to relax to equilibrium at high potentials when Pt^{2+} and PtO are in equilibrium. The model and experimental data indicated that at lower potentials (i.e., under the conditions of normal H_2/air fuel cell operation), the solubility of platinum in acid is quite low. At higher potentials on exposure to air to form PtO, the oxide layer effectively insulates the platinum particles from dissolution. At intermediate potentials, however, the uncovered surface is prone to high rates of platinum dissolution. Honji *et al.* [35, 41] found that the growth of platinum particles depends on their distribution on the carbon surface. They showed by TEM analysis that several platinum particles form a kind of colony. Table III shows the dependence of the number of platinum particles in the colony and particle size before and after sintering on platinum content in the catalyst. The number of Pt particles in the colony increases in a remarkable way with increasing platinum content, but

TABLE III Effect of platinum content in Pt/C catalysts on platinum particle dispersion [35]

Platinum content (wt%)	Number of particle in colony	Pt particle size before sintering (nm)	Pt particle size after sintering (nm)
5	2–5	3.8	5.6, 6.3
10	4–8	3.9, 4.4	7.8
13	6–10	3.8	7.3, 8.0
15	8–12	4.8	8.7, 9.0

the platinum particle size is about 4 nm, independent of platinum amount in the catalyst. In the hypothesis that the colony changes to form one particle, they estimated the platinum particle size after agglomeration by a simple calculation. The particle size after agglomeration D is given by the following equation in terms of the initial particle size D_o and the number of particles in colony N:

$$D = \left(N D_o^3\right)^{1/3} \tag{13}$$

Theoretical and experimental results were in good agreement, supporting this agglomeration model. As previously indicated, the use as dispersing agent of sorbitan monolaurate instead of polyoxyethylene glycol p-iso-octylphenyl ether, preventing the formation of Pt particle colonies, stabilises platinum particles against sintering [41]. A way to prevent the agglomeration of platinum particles was suggested by Bushnell and Jalan [78]. They found that the deposition of carbon on and around a carbon-supported platinum crystallite reduces Pt recrystallization.

The stability of carbon support affects the loss of platinum surface area following both platinum particle sintering and platinum release from the carbon support [37, 38, 79, 80]. The relation of carbon corrosion and platinum sintering was observed from TEM analysis by Gruver [79]. McBreen *et al.* [37] showed that Regal 660R carbon with a low volatile content and neutral pH stabilises platinum particles against sintering. Thermal treatment stabilises carbon against corrosion in hot phosphoric acid [79]. Uchida *et al.* [38] tested the durability of the carbon support in sulphuric acid solution at 60°C. The change in color of the sulphuric acid solution is indicative of carbon support dissolution. The colors from the furnace blacks were darker than those from the acetylene blacks, and those from carbon blacks with larger surface area were darker than those from carbon blacks with smaller surface area. The furnace blacks with the larger surface area had a tendency to be more soluble and unstable. The effect of thermal treatment at 370°C in air on the change in catalyst content during immersion in sulphuric acid solution is shown in Fig. 10. As it can be seen, heat treatment improved the stability of the catalysts in the sulphuric acid. Because of the thermal treatment, the carbon support hardly dissolved in the sulphuric acid solution and the solution was transparent.

The acid environment in the PEFCs is different from that of PAFCs. The anions of the perfluorinated sulfonic acid polymer are only weakly adsorbed on Pt, in contrast to the phosphoric anions, which are strongly

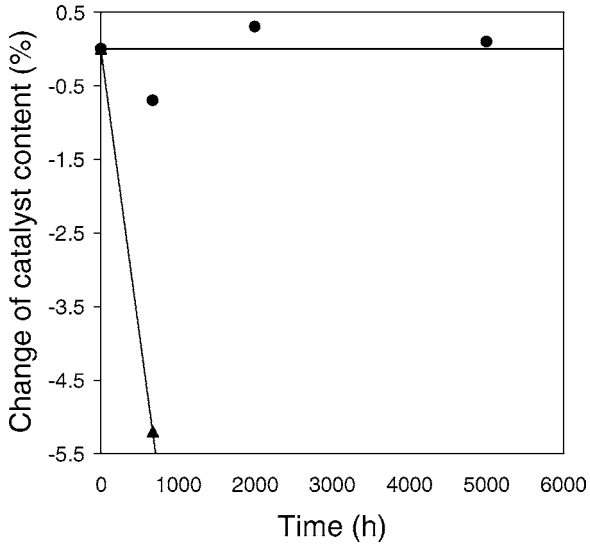

Figure 10 Catalyst loss vs. time of immersion in sulfuric acid solution: (▲) untreated electrode, (●) electrode heat treated at 370°C in air [38].

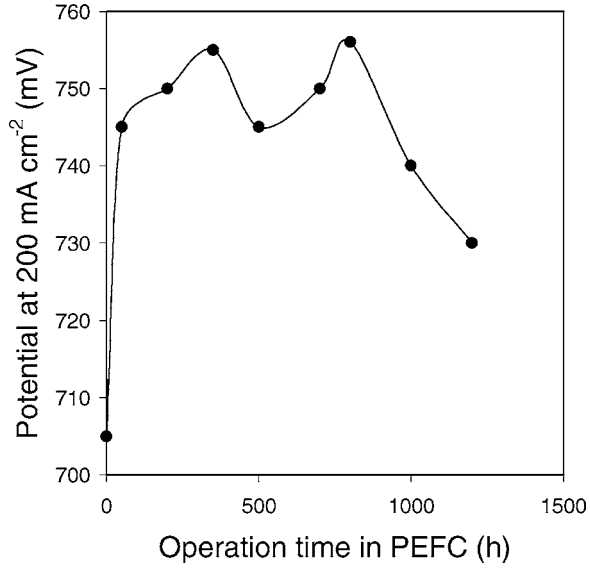

Figure 11 Lifetime evaluation of platinum catalyst for oxygen reduction in PEFC: current density 200 mA cm^{-2}; ambient pressure [81].

adsorbed. Furthermore, the PEFCs operates at less than 100°C, as compared with the PAFCs, which operates at twice this temperature. Then, a better stability of the catalyst in the PEFC environment is expected. Mukerjee and Srinivasan [81] evaluated the lifetime in single PEFC at a constant current density of 200 mA cm^{-2}. Considering the excellent stability of the Dow membrane, the lifetime of PEFC essentially depends on the catalyst stability. The cell potential, monitored over a time period of 1200 h, is shown in Fig. 11. A good stability of cell potential, and, as a consequence, of platinum particles up to 800 h, followed by a slow decrease in the performance of the cell, was observed.

5. Thermal stability

Bett *et al*. [75, 82] found a decrease in platinum surface area in N_2 or H_2 at temperatures higher than 600°C. Platinum is transferred from one crystallite to another by the migration of platinum atoms or by crystallite diffusion on the carbon surface. Table IV shows the effect of thermal treatment on particle size, determined by different techniques, of carbon-supported platinum alone [72] and after alloying with Co, Cr or Ni [83] (metal particle growth by alloying is negligible [1]). In all the cases, following heat treatment at temperature higher than 1000°C, the metal size was about four times larger than untreated Pt/C. At 1200°C, Bardi and Ross [84] denoted from hot-stage electron microscopy that Pt atom diffusion occurs resulting in particle size growth via Ostwald ripening. Fig. 12 shows the effect of the pH value during the impregnation of the metal precursor on carbon supported platinum on the Pt particle growth. As reported in [1], the slope of the lines and then the activation energy is lower at lower pH. It is known that the stability of the metal particles and the mechanism of platinum particle growth depend on the surface acid-base properties of the carbon support. The surface oxygen-containing functional groups may act as anchoring centres for the metal particles limiting their growth. The acidic/basic environment present on carbon surface during Pt/C impregnation with the precursor may modify the number and the characteristics of these anchoring centres, affecting in this way the movement of Pt particle on the carbon surface.

TABLE IV Metal particle size from both TEM and XRD measurements following different heat treatment temperature for Pt/C alone [72] and after alloy formation [83]

Heat treatment (°C)	Pt particle size (nm)		PtCo particle size (nm)		PtCr particle size (nm)		PtNi particle size (nm)	
	TEM	XRD	TEM	XRD	TEM	XRD	TEM	XRD
None	2.5		2.8[a]		2.8[a]		2.8[a]	
700			3.5	3.0	3.1	4.2	5.1	4.6
900	6.5		6.8	6.6	5.5	6.2	4.9	6.4
1100			10.9	8.6	8.6	10.4	11.0	10.2
1200	11.0	11.0						

[a]Pt/C starting material.

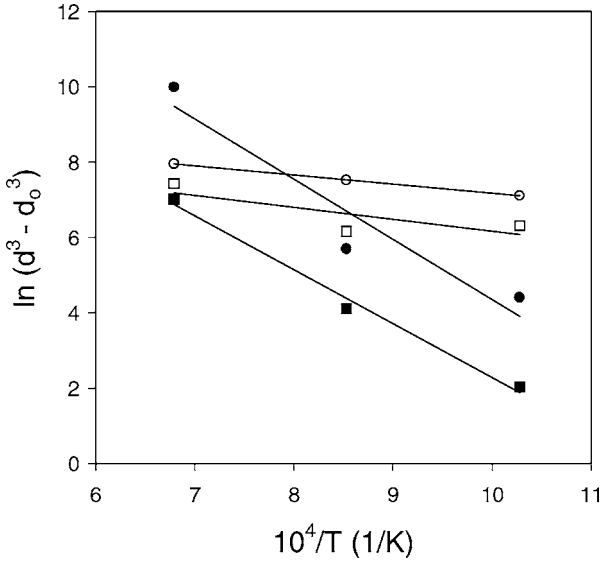

Figure 12 Arrhenius plots of PtCo and PtTi particle growth, prepared with different pH conditions [1]. ○, ● PtTi; □, ■ PtCo; ○, □ pH = 2; ●, ■ pH = 11.

6. Conclusions

An overview of the preparation methods of carbon-supported platinum and their correlation to microstructural characteristics and stability of the electrocatalyst has been attempted in this review to provide a guideline for future research. The method of preparation influences the choice of the carbon support and its pretreatment. The microscopic distribution of platinum on the carbon support, indeed, depends on the correspondence of the way of preparation and the characteristics of the substrate. Platinum amount and dispersity of Pt/C particles obtained by the impregnation method are related to the presence of oxygen sites on the carbon surface, while platinum distribution of Pt/C catalysts obtained by the colloidal method depends on reaction conditions such as choice of surface-active agents and synthesis temperature, and on the specific surface area of the carbon.

To improve Pt particle stability the following requirements have to be fulfilled, depending by the condition at which the catalyst is submitted:

(a) in fuel cell conditions → high platinum uniformity, low platinum content in the catalyst and/or carbon with high resistance to corrosion.

(b) thermal treatment at high temperatures → presence of basic groups on the carbon surface → strong anchoring.

In order to reduce the costs of the fuel cell system, electrodes with a significant lowering of Pt loading up to 0.1 mg cm^{-2} have been tested [85]. The use of these electrodes, to attain an effective cell performance, involves both a high platinum dispersity and an ability to sustain their microstructure for long times of cell operation. As a consequence, the method of preparation and the stability of carbon-supported platinum play an important role in the process of optimization of low-platinum loading electrodes for PAFCs and PEFCs.

References

1. E. ANTOLINI, *Mater. Chem. Phys.* **78** (2003) 563.
2. S. MUKERJEE, *J. Appl. Electrochem.* **20** (1990) 537.
3. F. RODRIGUEZ-REINOSO, *Carbon* **36** (1998) 159.
4. E. AUER, A. FREUND, J. PIETSCH and T. TACKE, *Appl. Catal.* A **173** (1998) 259.
5. L. B. OKHLOPKOVA, A. S. LISITSYN, V. A. LIKHOLOBOV, M. GURRATH and H. P. BOEHM, *ibid.* **204** (2000) 229.
6. M. A. FRAGA, E. JORDAO, M. J. MENDES, M. M. A. FREITAS, J. L. FARIA and J. L. FIGUEREDO, *J. Catal.* **209** (2002) 355.
7. E. CZARAN, J. FINSTER and K. H. SCHNABEL, *Z. Anorg. Allg. Chem.* **443** (1978) 175.
8. H. E. VAN DAM and H. VAN BEKKUM, *J. Catal.* **131** (1991) 335.
9. F. COLOMA, A. SEPULVEDA-ESCRIBANO, J. L. FIERRO and F. RODRIGUEZ-REINOSO, *Langmuir* **10** (1994) 750.
10. S. R. DE MIGUEL, O. A. SCELZA, M. C. ROMAN-MARTINEZ, C. SALINAS-MARTINEZ, D. CAZORLA-AMOROS and A. LINARES-SOLANO, *Appl. Catal.* A **170** (1998) 93.
11. G. C. TORRES, E. I. IABLONSKI, G. T. BARONETTI, A. A. CASTRO, S. R. DE MIGUEL, O. A. SCELZA, M. D. BLANCO, M. A. PENA JIMENEZ and J. L. G. FIERRO, *ibid.* **161** (1997) 213.
12. A. SEPULVEDA-ESCRIBANO, F. COLOMA and F. RODRIGUEZ-REINOSO, *ibid.* **173** (1998) 247.
13. P. J. CARROTT, M. M. CARROTT, A. J. CANDEIAS and J. P. RAMALO, *J. Chem. Soc. Faraday Trans.* **91** (1995) 2179.
14. A. POLANIA, E. PAPIRER, J. B. DONNETT and G. DAGOIS, *Carbon* **31** (1993) 473.
15. H. P. BOEHM, *ibid.* **32** (1994) 759.
16. M. V. LOPEZ-RAMON, F. STOEKLI, C. MORENO-CASTILLA and F. CARRASCO-MARIN, *ibid.* **37** (1999) 1215.
17. S. S. BARTON, M. J. B. EVANS, E. HALLIOP and J. A. F. MACDONALD, *ibid.* **35** (1997) 1361.
18. C. A. LEON, Y. LEON, J. M. SOLAR, V. CALEMMA and L. R. RADOVIC, *ibid.* **30** (1992) 797.
19. J. F. LAMBERT and M. CHE, *J. Mol. Catal.* A **162** (2000) 5.
20. M. C. ROMAN-MARTINEZ, D. CAZORLA-AMOROS, A. LINARES-SOLANO and C.S.M. LECEA, *Carbon* **33** (1995) 3.
21. S. R. MIGUEL, O. A. SCELZA, M. C. ROMAN-MARTINEZ, C. S. M. LECEA, D. CAZORLA-AMOROS and A. LINARES-SOLANO, *Appl. Catal.* A **170** (1998) 93.
22. L. D. AGEEVA, N. A. KOLPAKOVA, T. V. KOVYRKYNA, N. P. POTSYAPUN and A. S. BUINOVSKII, *J. Anal. Chem.* **56** (2001) 137.
23. D. S. CAMERON, S. J. COOPER, I. L. DODGSON, B. HARRISON and J. W. JENKINS, *Catal. Today* **7** (1990) 113.
24. C. PRADO-BURGUETE, A. LINARES-SOLANO, F. RODRIGUEZ-REINOSO and C. S. M. LECEA, *J. Catal.* **115** (1989) 98.
25. D. J. SUH, T. J. PARK and S. K. IHM, *Carbon* **31** (1993) 427.
26. P. EHRBURGER, O. P. MAJAHAN and P. L. JR. WALKER, *J. Catal.* **43** (1976) 61.
27. A. GUERRIERO-RUIZ, P. BADENES and I. RODRIGUEZ-RAMOS, *Appl. Catal.* A **173** (1998) 313.
28. M. WATANABE, M. UCHIDA and S. MOTOO, *J. Electroanal. Chem.* **229** (1987) 395.
29. H. G. PETROW and R. J. ALLEN, U.S. Patent no. 4,044,193 (1977).
30. E. ANTOLINI, L. GIORGI, F. CARDELLINI and E. PASSALACQUA, *J. Solid State Electrochem.* **5** (2001) 131.
31. N. GIORDANO, E. PASSALACQUA, L. PINO, A. S. ARICÒ, V. ANTONUCCI, M. VIVALDI and K. KINOSHITA, *Electrochimica Acta* **36** (1991) 1979.
32. Y. NAKAO and K. KAERIYAMA, *J. Colloid Interface Sci.* **110** (1986) 82.
33. D. DUFF, T. MALLAT, M. SCHNEIDER and A. BAIKER, *Appl. Catal.* A **133** (1995) 133.
34. N. TOSHIMA and K. HIRAKAWA, *Polym. J.* **31** (1999) 1127.
35. A. HONJI, T. MORI, K. TAMURA and Y. HISHINUMA, *J. Electrochem. Soc.* **135** (1988) 355.
36. X. WANG and I.-M. HSING, *Electrochimica Acta* **47** (2002) 2981.
37. J. MCBREEN, H. OLENDER, S. SRINIVASAN and K. KORDESCH, *J. Appl. Electrochem.* **11** (1981) 787.
38. M. UCHIDA, Y. AOYAMA, M. TANABE, N. YANAGIHARA, N. EDA and A. OHTA, *J. Electrochem. Soc.* **142** (1995) 2572.
39. M. WATANABE, H. SEI and P. STONEHART, *J. Electroanal. Chem.* **261** (1989) 375.
40. M. WATANABE, S. SAEGUSA and P. STONEHART, *Chem. Lett.* **9** (1989) 1487.
41. A. HONJI, T. MORI, K. TAMURA and Y. HISHINUMA, *J. Electrochem. Soc.* **137** (1990) 2084.
42. H. BONNEMANN, G. BRAUN, W. BRIJOUX, R. BRINKMANN, A. TILLING, K. SEEVOGEL and K. SIEPEN, *J. Organomet. Chem.* **520** (1996) 143.
43. A. STOYANOVA, V. NAIDENOV, K. PETROV, I. NIKOLOV, T. VITANOV and E. BUDEVSKI, *J. Appl. Electrochem.* **29** (1999) 1197.
44. K. TSURUMI, T. NAKAMURA and A. SATO, U.S. Patent no. 4,956,331 (1990).

45. E. ANTOLINI, F. CARDELLINI, E. GIACOMETTI and G. SQUADRITO, *J. Mater. Sci.* **37** (2002) 133.
46. T. TORRE, A. S. ARICÒ, V. ALDERUCCI, V. ANTONUCCI and N. GIORDANO, *Appl. Catal.* A **114** (1994) 257.
47. V. M. JALAN and C. L. BUSHNELL, U.S. Patent no. 4,136,056 (1979).
48. V. M. JALAN, in "Extended Abstracts, Meeting Electrochemical Society" (Montreal, Canada, 1982).
49. M. VAARKAMP, J. T. MILLER, F. S. MODICA, G. S. LANE and D. C. KONINGBERGER, *J. Catal.* **138** (1992) 675.
50. S. C. ROY, P. A. CHRISTENSEN, A. HAMNETT, K. M. THOMAS and V. TRAPP, *J. Electrochem. Soc.* **143** (1996) 3073.
51. S. MUKERJEE, S. SRINIVASAN, M. P. SORIAGA and J. MCBREEN, *ibid.* **142** (1995) 1409.
52. A. PEBLER, *ibid.* **133** (1986) 9.
53. I. J. HILLENBRAND and J. W. LACKSONEN, *ibid.* **112** (1965) 249.
54. J. ESCARD, C. LECLERC and J. P. CONTOUR, *J. Catal.* **29** (1973) 31.
55. J. C. VEDRINE, M. DUFAUX, C. NACCACHE and B. IMELIK, *J. Chem. Soc. Faraday Trans.* **74** (1978) 440.
56. A. K. SHUKLA, M. K. RAVIKUMAR, A. ROY, S. R. BARMAN, D. D. SARMA, A. S. ARICÒ, V. ANTONUCCI, L. PINO and N. GIORDANO, *J. Electrochem. Soc.* **141** (1994) 1517.
57. K. L. MITTAL, *J. Vac. Sci. Technol.* **13** (1976) 19.
58. M. G. MASON, *Phys. Rev.* B **27** (1983) 748.
59. T. T. P. CHEUNG, *Surf. Sci.* **140** (1984) 151.
60. W. EBERHARDT, P. FAYET, D. M. COX, Z. FU, A. KALDOR, R. SHERWOOD and D. SONDERICKER, *Phys. Rev. Lett.* **64** (1990) 780.
61. K. KINOSHITA, *J. Electrochem. Soc.* **137** (1990) 845.
62. W. ROMANOWSKI, *Surf. Sci.* **18** (1969) 373.
63. V. M. JALAN, in "Extended Abstracts" (Meeting Electrochemical Society, Los Angeles, CA, 1979).
64. M. L. SATTLER and P. N. ROSS, *Ultramicroscopy* **20** (1986) 21.
65. M. KOMIYAMA, J. KOBAYASHI and S. MORICA, *J. Vac. Sci. Tech.* **8** (1990) 608.
66. R. VAN HARDEVELD and A. VAN MONTFOORT, *Surf. Sci.* **4** (1966) 396.
67. R. VAN HARDEVELD and F. HARTOG, *ibid.* **15** (1969) 189.
68. A. C. C. TSEUNG and S. C. DHARA, *Electrochimica Acta* **20** (1975) 681.
69. K. F. BLURTON, H. R. KUNZ and D. R. RUTT, *ibid.* **23** (1978) 183.
70. P. BINDRA, S. CLOUSER and E. YEAGER, *J. Electrochem. Soc.* **126** (1979) 1631.
71. G. A. GLUVER, R. F. PASCOE and H. R. KUNZ, *ibid.* **127** (1980) 1219.
72. B. C. BEARD and P. N. ROSS, *ibid.* **137** (1990) 3368.
73. M. POURBAIX, "Atlas of Electrochemical Equilibrium in Aqueous Solutions," 1st ed. (Pergamon Press, Bristol, England, 1966).
74. P. J. HYDE, C. J. MAGGIORE and S. SRINIVASAN, *J. Electroanal. Chem.* **168** (1984) 383.
75. J. A. BETT, K. KINOSHITA and P. STONEHART, *J. Catal.* **41** (1976) 124.
76. P. STONEHART and P. A. ZUCKS, *Electrochimica Acta* **17** (1972) 2333.
77. J. P. MEYERS and R. M. DARLING, in "Extended Abstracts" (Meeting Electrochemical Society, Salt Lake City, UT, 2002).
78. C. L. BUSHNELL and V. M. JALAN, U.S. Patent no. 4,137,372, (1979).
79. G. A. GRUVER, *J. Electrochem. Soc.* **125** (1978) 1719.
80. P. STONEHART, *Carbon* **22** (1984) 423.
81. S. MUKERJEE and S. SRINIVASANs *J. Electroanal. Chem.* **357** (1993) 201.
82. J. A. BETT, K. KINOSHITA and P. STONEHART, *J. Catal.* **35** (1974) 307.
83. M. MIN, J. CHO, K. CHO and H. KIM, *Electrochimica Acta* **45** (2000) 4211.
84. U. BARDI and P. N. ROSS, *J. Vac. Sci. Technol.* A **2** (1984) 1461.
85. L. GIORGI, E. ANTOLINI, A. POZIO and E. PASSALACQUA, *Electrochimica Acta* **43** (1998) 3675.

Received 25 January 2003
and accepted 17 April 2003